World Academy of Science, Engineering and Technology
International Journal of Mechanical and Mechatronics Engineering
Vol:3, No:12, 2009

Effect of Groove Location on the Dynamic Characteristics of Multiple Axial Groove Water Lubricated Journal Bearing

M. Vijaya Kini, R. S. Pai, D. Srikanth Rao, Satish Shenoy B and R. Pai

***Abstract*—**The stability characteristics of water lubricated journal bearings having three axial grooves are obtained theoretically. In this lubricant (water) is fed under pressure from one end of the bearing, through the 3-axial grooves (groove angles may vary). These bearings can use the process fluid as the lubricant, as in the case of feed water pumps.

The Reynolds equation is solved numerically by the finite difference method satisfying the boundary conditions. The stiffness and damping coefficient for various bearing number and eccentricity ratios, assuming linear pressure drop along the groove, shows that smaller groove angles better results.

***Keywords*—**3-axial groove, dynamic characteristics, groove location, water lubricated bearings.

I. INTRODUCTION

THE stability of a three axial groove water lubricated journal bearing is studied theoretically. In multiple axial grooved bearings one of the best ways of supplying the lubricant is through the axial groove. Such grooves are preferred when the cooling effect due to the flow of lubricant becomes critical. When pressurized lubricant is fed through the axial groove, the flow rate increases which plays an important role in maintaining an uninterrupted water film and removing most of the frictional heat. In this study, lubricant is fed under pressure from one end of the bearing, through three axial grooves (groove angle may vary) and around the clearance between the shaft and the bearing bush. The flow in this region will be both circumferential and axial [1]. The provision of grooves should not be in the load carrying area and should be close to the maximum film thickness which would least interfere with the hydrodynamic performance of the bearing. This would provide maximum performance [2]. Flow through bearings depends on viscosity of the lubricant, bearing clearance and lubricant supply system. Shelly and Ettles [3] discovered that positioning the grooves at the maximum pressure location will cause 30 to 70 percent reduction in the load capacity of the bearing. This results in the lowering of the film thickness between journal and bearing which could lead to journal bearing contact and hence increased wear [4]. The provision of the grooves should not be in the load carrying area and should be as close to the maximum film thickness which would least interfere with the hydrodynamic performance of the bearing. This would provide maximum performance[5].

Water lubricated bearings would represent an environmentally acceptable option because there is no pollution. Therefore water lubricated applications are expected to continue to grow and a complete bearing design must examine all aspects of the bearing performance.

The Reynolds equation in two dimensions for incompressible fluid is solved numerically by finite difference method. The dynamic characteristics are obtained in terms of stiffness and damping coefficient using a first-order-perturbation method to ascertain the stability of the bearing system.

The dynamic characteristics are studied for 12°and 36° groove angles and with JFO boundary conditions. Typical results obtained are presented in the form of charts, which can be used conveniently in the design of such bearings as these are presented in dimensionless form. The results are compared with those obtained with Reynolds boundaries.

M.Vijaya Kini, is with the Manipal Institute of Technology, Manipal, INDIA (phone: +91 820 2925462; fax: +91 820 2571071; e-mail: mvkini@yahoo.com).

Ramamohan S Pai, is with the Manipal Institute of Technology, Manipal, INDIA (phone: +91 820 2925462; fax: +91 820 2571071; e-mail: rammohan_pai@yahoo.com).

D.Srikanth Rao is with the Manipal Institute of Technology, Manipal, INDIA (phone: +91 820 2925462; fax: +91 820 2571071; e-mail: dassrao@yahoo.com).

Satish Shenoy B**,** is with the Manipal Institute of Technology, Manipal, INDIA (phone: +91 820 2925462; fax: +91 820 2571071; e-mail: satishshenoyb@yahoo.com).

Raghuvir Pai B, is with the Manipal Institute of Technology, Manipal, INDIA (phone: +91 820 2925462; fax: +91 820 2571071; e-mail: rbpai@yahoo.com).

II. THEORY

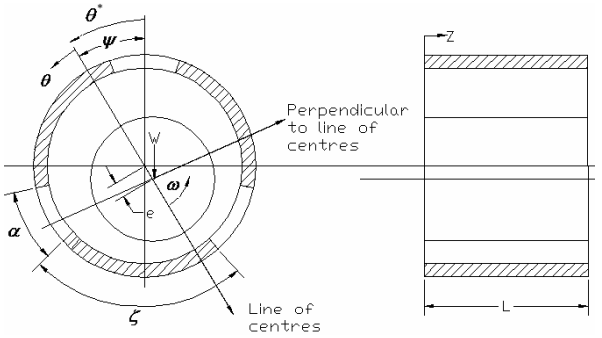

Fig. 1 Three axial groove journal bearing and the coordinate system.

The Reynolds equation under dynamic condition is:

$$\frac{\partial}{\partial \vartheta}\left(\bar{h}^3 \frac{\partial \bar{p}}{\partial \theta}\right)+\frac{1}{4}\left(\frac{D}{L}\right)^2 \bar{h}^3 \frac{\partial^2 \bar{p}}{\partial \bar{z}^2}=\Lambda \frac{d\bar{h}}{d\theta}+2\Lambda\lambda \frac{\partial \bar{h}}{\partial \tau} \tag{1}$$

Boundary conditions

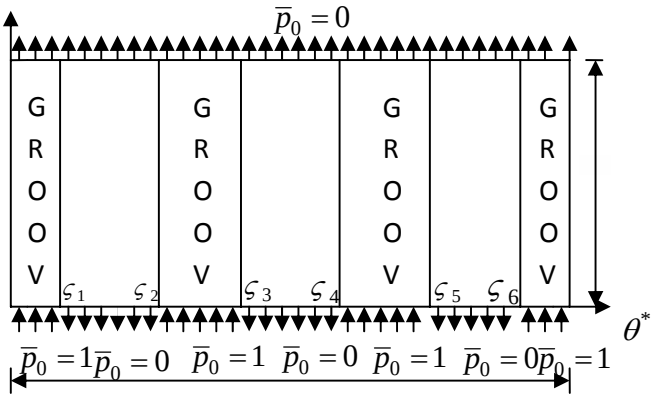

Fig. 2 Developed view of the bearing showing the boundary conditions.

The domain boundary conditions for the five axial grooved journal bearing are given below.

$\bar{p}_0 = 1$ at $\bar{z} = 0$ at the grooves and elsewhere $\bar{p}_0 = 0$

and $\bar{p}_0 = 0$ at $\bar{z} = 1$ for all θ

$$\bar{p} = 0,\ \partial \bar{p}/\partial \theta = 0 \tag{2}$$

The journal performs a periodic motion of small amplitude $\mathrm{Re}\left(C\varepsilon_1 e^{i\tau}\right)$ along the line of centers and $\mathrm{Re}\left(C\varepsilon_0\phi_1 e^{i\tau}\right)$ perpendicular to the line of centers around its steady state position ε_0 and ϕ_0.

It is assumed that at the onset of instability, the position of the journal center can be defined as a steady state value (ε_0, ϕ_0) together with a harmonic vibration of

frequency ω_p, thus

$$\varepsilon = \varepsilon_0 + \varepsilon_1 e^{i\tau}$$

$$\phi = \phi_0 + \phi_1 e^{i\tau}$$

$$|\varepsilon_1| \langle\langle \varepsilon_0$$

where

$$|\phi_1| \langle\langle \phi_0$$

Under this condition (i.e. for small amplitude of vibration) first - order perturbation will be valid. The pressure and film thickness can be written as:

$$\bar{p} = \bar{p}_0 + \varepsilon_1 e^{i\tau}\bar{p}_1 + \varepsilon_0\phi_1 e^{i\tau}\bar{p}_2 \tag{3}$$

$$\bar{h} = \bar{h}_0 + \varepsilon_1 e^{i\tau}\cos\theta + \varepsilon_0\phi_1 e^{i\tau}\sin\theta \tag{4}$$

Substitution of equations (3) and (4) into equation (1) and retaining up to first linear terms, we get the following three equations:

$$\varepsilon_0 : \bar{h}_0^3 \frac{\partial^2 \bar{p}_0}{\partial\theta^2} + 3.0\bar{h}_0^2 \frac{\partial \bar{h}_0}{\partial\theta}\frac{\partial \bar{p}_0}{\partial\theta} + \frac{1}{4}\left(\frac{D}{L}\right)^2 \bar{h}_0^3 \frac{\partial^2 \bar{p}_0}{\partial \bar{z}^2} - \Lambda\frac{d\bar{h}_0}{d\theta} = 0 \tag{5}$$

$$\begin{aligned}\varepsilon_1 e^{i\tau} : {} & \bar{h}_0^3 \frac{\partial^2 \bar{p}_1}{\partial\theta^2} + 3.0\bar{h}_0^2\cos\theta\frac{\partial^2 \bar{p}_0}{\partial\theta^2} - 3.0\bar{h}_0^2\sin\theta\frac{\partial \bar{p}_0}{\partial\theta} + 6.0\bar{h}_0\cos\theta\frac{\partial \bar{h}_0}{\partial\theta}\frac{\partial \bar{p}_0}{\partial\theta} \\ & + 3.0\bar{h}_0^2\frac{\partial \bar{h}_0}{\partial\theta}\frac{\partial \bar{p}_1}{\partial\theta} + \frac{1}{4}\left(\frac{D}{L}\right)^2 \bar{h}_0^3 \frac{\partial^2 \bar{p}_1}{\partial \bar{z}^2} + \frac{3}{4}\left(\frac{D}{L}\right)^2 \bar{h}_0^2\cos\theta\frac{\partial^2 \bar{p}_0}{\partial \bar{z}^2} \\ & + \Lambda\sin\theta - 2i\Lambda\lambda\sin\theta = 0\end{aligned} \tag{6}$$

$$\begin{aligned}\varepsilon_0\phi_1 e^{i\tau} : {} & \bar{h}_0^3 \frac{\partial^2 \bar{p}_2}{\partial\theta^2} + 3.0\bar{h}_0^2\sin\theta\frac{\partial^2 \bar{p}_0}{\partial\theta^2} + 3.0\bar{h}_0^2\cos\theta\frac{\partial \bar{p}_0}{\partial\theta} + 6.0\bar{h}_0\sin\theta\frac{\partial \bar{h}_0}{\partial\theta}\frac{\partial \bar{p}_0}{\partial\theta} \\ & + 3.0\bar{h}_0^2\frac{\partial \bar{h}_0}{\partial\theta}\frac{\partial \bar{p}_2}{\partial\theta} + \frac{1}{4}\left(\frac{D}{L}\right)^2 \bar{h}_0^3 \frac{\partial^2 \bar{p}_2}{\partial \bar{z}^2} + \frac{3}{4}\left(\frac{D}{L}\right)^2 \bar{h}_0^2\sin\theta\frac{\partial^2 \bar{p}_0}{\partial \bar{z}^2} \\ & - \Lambda\cos\theta - 2i\Lambda\lambda.\sin\theta = 0\end{aligned} \tag{7}$$

as shown in Fig. 2.

Knowing the steady state pressure distribution equations (6) and (7) are solved numerically satisfying the modified boundary conditions of equation (2).

A. Stiffness and Damping coefficients

The dynamic pressures p_1 and p_2 are produced due to the dynamic displacements of the journal center $\mathrm{Re}\left(C\varepsilon_1 e^{i\tau}\right)$ parallel to and $\mathrm{Re}\left(C\varepsilon_0\phi_1 e^{i\tau}\right)$ perpendicular to the line of centers. The components of the dynamic load due to the

dynamic pressure p_1 along and perpendicular to the line of centers can be written as:

$$(W_1)_r = \int_0^L \int_0^{2\pi} p_1 R.\cos\theta.d\theta.dz$$

$$(W_1)_\phi = \int_0^L \int_0^{2\pi} p_1 R.\sin\theta.d\theta.dz \quad (8)$$

It is treated that the fluid film, which supports the rotor, is equivalent to a spring and a dashpot system. Since the journal executes small harmonic oscillation about its steady state position, the dynamic load carrying capacity can be expressed as a spring and a viscous damping force as given below:

$$-(W_1)_r \varepsilon_1 e^{i\tau} = K_{rr} Y + D_{rr} \frac{dY}{dt}$$

$$-(W_1)_\phi \varepsilon_1 e^{i\tau} = K_{\phi r} Y + D_{\phi r} \frac{dY}{dt} \quad (9)$$

where the position of the journal centre is given by $Y = C\varepsilon_1 e^{i\tau}$

Now,

$$(\overline{W_1})_r = \frac{(W_1)_r}{LDp_s} = \int_o^1 \int_0^{2\pi} \overline{p}_1.\cos\theta.d\theta.d\overline{z} \quad (10)$$

$$(\overline{W_1})_\phi = \frac{(W_1)_\phi}{LDp_s} = \int_0^1 \int_0^{2\pi} \overline{p}_1.\sin\theta.d\theta.d\overline{z} \quad (11)$$

Using equation (10) and (11), we can write

$$-(\overline{W_1})_r = -\int_0^1 \int_0^{2\pi} \overline{p}_1.\cos\theta.d\theta.d\overline{z} = \frac{K_{rr}C}{LDp_s} + i\frac{D_{rr}C\omega_p}{LDp_s}$$

$$-(\overline{W_1})_\phi = -\int_0^1 \int_0^{2\pi} \overline{p}_1.\sin\theta.d\theta.d\overline{z} = \frac{K_{\phi r}C}{LDp_s} + i\frac{D_{\phi r}C\omega_p}{LDp_s} \quad (12)$$

Since p_1 is complex, the dynamic load $\overline{W_1}$ can be expressed in terms of real and imaginary parts as

$$\overline{W_1} = \mathrm{Re}(\overline{W_1}) + i\,\mathrm{Im}(\overline{W_1}) \quad (13)$$

Hence we get,

$$\overline{K}_{rr} = -\mathrm{Re}\left[\int_0^1 \int_0^{2\pi} \overline{p}_1.\cos\theta.d\theta.d\overline{z}\right]$$

$$\overline{K}_{\phi r} = -\mathrm{Re}\left[\int_0^1 \int_0^{2\pi} \overline{p}_1.\sin\theta.d\theta.d\overline{z}\right] \quad (14)$$

$$\overline{D}_{rr} = -\mathrm{Im}\left[\int_0^1 \int_0^{2\pi} \overline{p}_1.\cos\theta.d\theta.d\overline{z}\right] \Big/ \lambda$$

$$\overline{D}_{\phi r} = -\mathrm{Im}\left[\int_0^1 \int_0^{2\pi} \overline{p}_1.\sin\theta.d\theta.d\overline{z}\right] \Big/ \lambda$$

where, $\overline{K}_{ij} = \frac{K_{ij}C}{LDp_s}$ and $\overline{D}_{ij} = \frac{D_{ij}C\omega}{LDp_s}$

Similarly, considering the dynamic displacement of the journal centre along ϕ direction, the following expressions results.

$$\overline{K}_{\phi\phi} = -\mathrm{Re}\left[\int_0^1 \int_0^{2\pi} \overline{p}_2.\sin\theta.d\theta.d\overline{z}\right]$$

$$\overline{K}_{r\phi} = -\mathrm{Re}\left[\int_0^1 \int_0^{2\pi} \overline{p}_2.\cos\theta.d\theta.d\overline{z}\right] \quad (15)$$

$$\overline{D}_{\phi\phi} = -\mathrm{Im}\left[\int_0^1 \int_0^{2\pi} \overline{p}_2.\sin\theta.d\theta.d\overline{z}\right] \Big/ \lambda$$

$$\overline{D}_{r\phi} = -\mathrm{Im}\left[\int_0^1 \int_0^{2\pi} \overline{p}_2.\cos\theta.d\theta.d\overline{z}\right] \Big/ \lambda$$

The stiffness and damping coefficients thus obtained can be used to study the stability of a rigid rotor.

$$\overline{M} = \frac{1}{\lambda^2(\overline{D}_{\phi\phi} + \overline{D}_{rr})}\left[(\overline{D}_{rr}\overline{K}_{\phi\phi} + \overline{K}_{rr}\overline{D}_{\phi\phi}) - (\overline{K}_{\phi r}\overline{D}_{r\phi} + \overline{D}_{\phi r}\overline{K}_{r\phi}) + \frac{\overline{W}}{\varepsilon_0}(\overline{D}_{rr}\cos\phi_0 - \overline{D}_{\phi r}\sin\phi_0)\right] \quad (16)$$

$$\overline{M}^2\lambda^4 - \lambda^2\left[\overline{M}\left(\frac{\overline{W}\cos\phi_0}{\varepsilon_0} + \overline{K}_{\phi\phi} + \overline{K}_{rr}\right) + (\overline{D}_{rr}\overline{D}_{\phi\phi} - \overline{D}_{\phi r}\overline{D}_{r\phi})\right] + (\overline{K}_{rr}\overline{K}_{\phi\phi} - \overline{K}_{\phi r}\overline{K}_{r\phi}) + \frac{\overline{W}}{\varepsilon_0}(\overline{K}_{rr}\cos\phi_0 - \overline{K}_{\phi r}\sin\phi_0) = 0 \quad (17)$$

III. RESULTS AND DISCUSSIONS

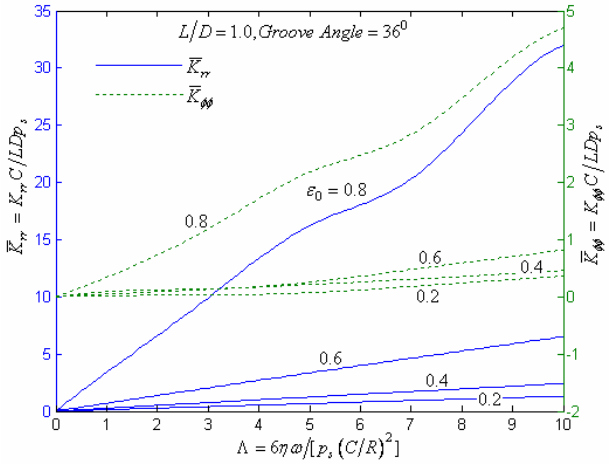

Fig. 3 Variation of direct stiffness coefficient with Λ for various ε_0

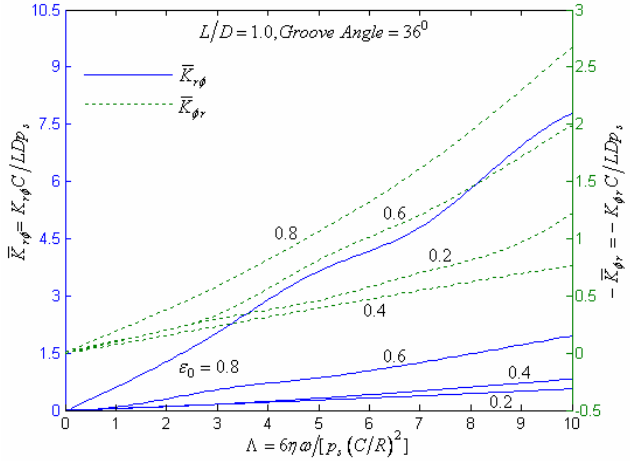

Fig. 4 Variation of cross stiffness coefficient with Λ for various ε_0

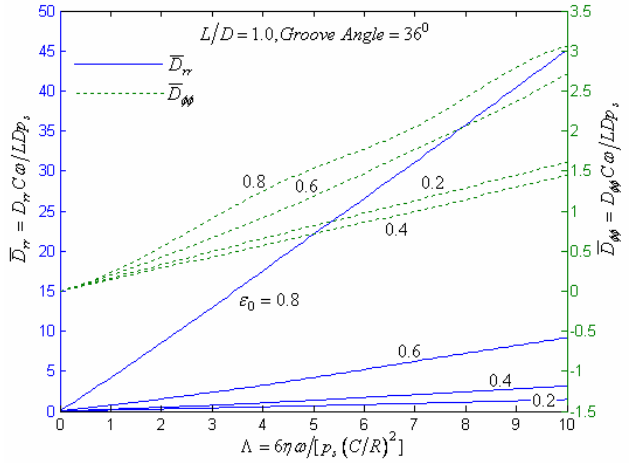

Fig. 5 Variation of direct damping coefficient with Λ for various ε_0

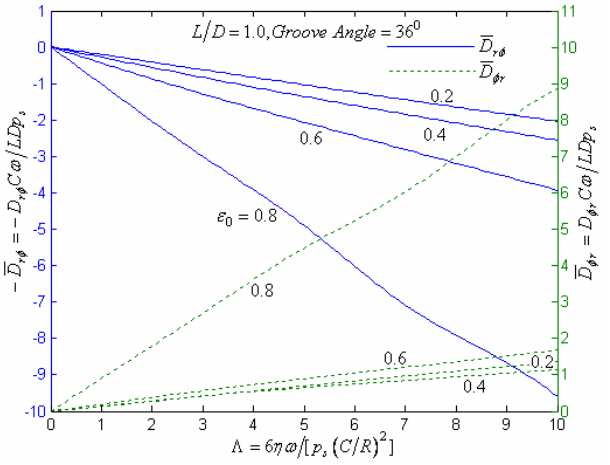

Fig. 6 Variation of cross damping coefficient with Λ for various ε_0

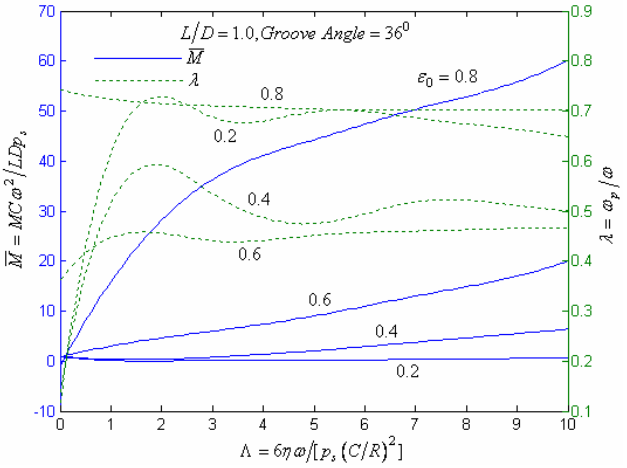

Fig. 7 Variation of stability and whirl with Λ for various ε_0

TABLE I
COMPARISON OF RESULTS OF 36^0 AND 12^0 ANGLE GROOVED BEARINGS (L/D =1.0, Λ = 10, LINEAR PRESSURE DROP)

ε_0	Groove Angle	$\overline{M}$	λ
0.2	12^0	1.8040	0.6127
	36^0	0.6793	0.6487
0.4	12^0	11.5979	0.5796
	36^0	6.3822	0.5128
0.6	12^0	52.9772	0.4831
	36^0	32.4432	0.4692

0.8	12^0	85.9303	0.6811
	36^0	60.2443	0.7101

Table 1. Comparison of results of 36^0 and 12^0 angle grooved bearings (L/D =1.0, Λ = 10, linear pressure drop)

Stiffness and damping coefficients are shown in Fig 3 – 7 for various eccentricity ratios and speed parameters. It has been observed that these coefficients, except $\overline{D}_{r\phi}$, increase with an increase in journal speed. It can be seen that $\overline{K}_{\phi r}$ and $\overline{D}_{r\phi}$ (Figs 4 and Fig. 6) have negative values. The stiffness and damping coefficients are mainly responsible for the whirl instability of the bearing. The effect of an individual coefficient on the speed and eccentricity ratio may not indicate the trend of stability characteristics. These coefficients do not give much of a basis for comparing various bearing designs with one another. However, these are quite useful for the calculation of threshold speed.

The speed of journal calculated from the value of $\overline{M}$ is the threshold speed, above which the bearing system will be unstable. The whirl speed (speed of the journal centre) can be found from the whirl ratio for the above journal speed. Fig. 5 shows the variation in mass parameter $\overline{M}$ and whirl ratio λ (the measure of stability). The upper portion of the curve for $\overline{M}$ is the unstable region and the lower portion one is the stable region.

It can be seen that the results are better for smaller groove angles when compared with the 36^0 groove angle (Table 1).

IV. CONCLUSIONS

From the above study we can conclude that:

1. The considerable change in the mass parameter for 12^0 groove angle shows improved stability when compared to 36^0 groove angles. It is therefore, preferable to use a smaller groove angle.
2. The data obtained from the above analysis can be used conveniently in the design of water lubricated journal bearings, as these are presented in dimensionless form.

TABLE II
NOMENCLATURE

Symbol	Name
C	Radial clearance (m)
D	Diameter of the bearing (m)
$D_{rr}, D_{\phi\phi}, D_{r\phi}, D_{\phi r}$	Damping coefficients (Ns/m)
$\overline{D}_{rr}, \overline{D}_{\phi\phi}, \overline{D}_{r\phi}, \overline{D}_{\phi r}$	Nondimensional damping coefficients, $\overline{D}_{ij} = D_{ij}C\omega / LDp_s$
$K_{rr}, K_{\phi\phi}, K_{r\phi}, K_{\phi r}$	Stiffness coefficients (N/m)
$\overline{K}_{rr}, \overline{K}_{\phi\phi}, \overline{K}_{r\phi}\overline{K}_{\phi r}$	Nondimensional stiffness coefficients, $\overline{K}_{ij} = K_{ij}C / LDp_s$
L	Length of the bearing (m)
$\overline{p}_0$	Pressure at the bearing edges
$\overline{p}_1, \overline{p}_2$	Perturbed pressures
R	Journal radius (m)
t	Time (s)
U	Journal peripheral speed, ωR
α	Groove angle (rad.)
ε_1, ϕ_1	Perturbation parameters
η	Coefficient of absolute viscosity of the lubricant (N s/m^2)
$\theta, \bar{z}$	Nondimensional co-ordinates, $\theta = x/R, \bar{z} = z/L$, θ measured from the line of centres.
θ^*	Co-ordinate in the circumferential direction measured from centre of the groove.
λ	Whirl ratio, ω_p / ω
$\varsigma_1, \varsigma_3, \varsigma_5, \varsigma_7, \varsigma_9, \varsigma_{11}$	Inlet angle of the lobes
$\varsigma_2, \varsigma_4, \varsigma_6, \varsigma_8, \varsigma_{10}, \varsigma_{12}$	Outlet angle of the lobes
ξ	Lobe angle (rad.)
Λ	Bearing number, $6\eta\omega / [p_s (C/R)^2]$
τ	Nondimensional time, $\omega_p t$
ϕ, ϕ_0	Attitude angle (rad)
ω	Journal rotational speed (rad /s)

REFERENCES

[1] B.C.Majumdar, R. Pai, and D. J. Hargreaves, "Analysis of water lubricated Journal Bearings with Multiple axial grooves". Proc. Instn. Mech. Engrs, Part J, Journal of Engineering Tribology, Vol. 218, 2004, pp. 135-146.

[2] R. Pai,, and B.C.Majumdar, "Stability of submerged oil film journal bearings under dynamic load". Wear, Vol. 146, 1991, pp. 125 - 135.

[3] Shelly, P and Ettles, C., "Solutions for the load capacity of journal bearings with oil grooves, Holes, Reliefs or Chamfers in Non - optimum positions". Proc.Instn Mech. Engrs, 1971, C56/71, pp. 38-46.

[4] D. J. Hargreaves, and Elgezway, A.S., "Optimization of grooving arrangements in water lubricated Non-Metallic journal bearings". Trans. IEAust, ME18 (3), 1993, pp. 245 - 251.

[5] Vijayaraghavan, D., and Keith, T.G. "Effect of type of location of oil groove on the performance of journal bearings". Tribology Trans, 35, 1992, pp. 98-106.